IOPscience iopscience.iop.org

Home Search Collections Journals About Contact us My IOPscience

The coercivity of the melt-spun Sm-Fe-Ga-C permanent magnets and the effect of additives (Nb, Cu and Zr)

This article has been downloaded from IOPscience. Please scroll down to see the full text article.

2001 J. Phys.: Condens. Matter 13 10487

(http://iopscience.iop.org/0953-8984/13/46/317)

View the table of contents for this issue, or go to the journal homepage for more

Download details:
IP Address: 171.66.16.226
The article was downloaded on 16/05/2010 at 15:10

Please note that terms and conditions apply.

INSTITUTE OF PHYSICS PUBLISHING JOURNAL OF PHYSICS: CONDENSED MATTER

J. Phys.: Condens. Matter **13** (2001) 10487–10496 PII: S0953-8984(01)23046-X

The coercivity of the melt-spun Sm–Fe–Ga–C permanent magnets and the effect of additives (Nb, Cu and Zr)

Junxian Zhang[1], **I Kleinschroth, D Goll, F Cuevas and H Kronmüller**

Max-Planck-Institut für Metallforschung, Heisenbergstrasse 1, D-70569 Stuttgart, Germany

E-mail: zhang@glvt-cnrs.fr

Received 16 March 2001, in final form 20 June 2001
Published 2 November 2001
Online at stacks.iop.org/JPhysCM/13/10487

Abstract

$Sm_2Fe_{15}Ga_2C_3$ and $Sm_2Fe_{15}Ga_2M_{0.2}C_3$ (M = Nb, Cu, Zr) ribbons with Th_2Zn_{17}-type structure have been synthesized by melt-spinning and subsequent annealing at temperatures above 1023 K. A nanoscale 2:17 phase with grain sizes of 50–200 nm is developed. The anisotropy constants K_1 and K_2 are determined in the temperature range of 150–600 K by fitting the demagnetization curve of the isotropic samples. Furthermore, the intrinsic material parameters, like the Curie temperature, exchange constant, anisotropy field and critical diameter of single domain particles are given. In order to understand the magnetic hardening mechanism, the temperature dependence of the coercivity is analysed within the framework of the micromagnetic models. It is concluded that the magnetic hardening mechanism at low temperatures up to 350 K is dominated by nucleation processes in a magnetically inhomogeneous region. The average widths of the inhomogeneities of 2 nm and 3 nm for $Sm_2Fe_{15}Ga_2C_3$ and $Sm_2Fe_{15}Ga_2M_{0.2}C_3$ (M = Nb, Cu, Zr) are determined, respectively. At high temperature the pinning of the domain walls by grain boundaries controls the coercivity mechanism.

1. Introduction

Coercivity is one of the most important features of a permanent magnet. It must be noted that the coercivity is not an intrinsic magnetic property, which means that the coercivity depends not only on the anisotropy and the spontaneous magnetization, but also depends on the microstructure of the materials. Owing to scientific and technological interests, the coercivity mechanisms of rare earth permanent magnets have attracted much attention recently [1–4]. The micromagnetic model, which was developed by Kronmüller and co-workers, has been applied successfully to rare earth permanents magnet during the last two decades [5–8]. Concerning

[1] Corresponding author.

0953-8984/01/4610487+10$30.00 © 2001 IOP Publishing Ltd Printed in the UK

the magnetization reversal process of rare earth permanent magnets, two different coercivity mechanisms have been established: nucleation and pinning. For nucleation, the coercivity corresponds to the applied inverse field strength required to nucleate reversed domains. The pinning coercivity mechanism is controlled by the domain wall propagation process, where it is assumed that reversed domains can nucleate at low fields. In this case, the coercivity corresponds to the applied inverse field required to move a domain wall over the maximum potential barrier. In order to apply the micromagnetic analysis to the coercivity mechanism, it is a prerequisite to know the intrinsic magnetic parameters.

$Sm_2(Fe,Ga)_{17}C_x$ compounds are suitable candidates as permanent magnets, because of their high thermal stability and their excellent intrinsic magnetic properties exhibiting a Curie temperature of $T_C \approx 620$ K, a magnetic saturation polarization of $J_s \approx 1.0$ T and a magnetocrystalline anisotropy field of $H_a \approx 12$ T [9]. High coercivities of 1.2–1.6 T have been achieved in $Sm_2Fe_{15}Ga_2C_x$ nanocrystalline alloys [10, 11]. However the magnetic hardening mechanism has rarely been studied. For mechanically alloyed $Sm_2Fe_{17}N_x$ magnets, Ding *et al* [12] suggested the pinning mechanism whereas Kou *et al* [13] proposed that the nucleation process governs the coercivity. For melt spun $Sm_2(Fe,Ga)_{17}C_x$ compounds, Shen *et al* [14] have reported that a nucleation process in the temperature range 5–300 K exists. In this paper a small amount of additives M = Cu, Nb and Zr is added to $Sm_2Fe_{15}Ga_2C_3$ magnets in order to modify the hard magnetic properties. The intrinsic magnetic properties of these materials have been determined. The remainder of the paper will be devoted to the coercivity mechanism analysis of the temperature dependence of the coercivity.

2. Experimental procedure

Alloys with nominal composition $Sm_2Fe_{15}Ga_2C_3$ and $Sm_2Fe_{15}Ga_2M_{0.2}C_3$ (M = Nb, Cu, Zr) were prepared by arc melting in a high purity argon atmosphere. The ribbons, with a width of about 2.5 mm and a thickness of 30 μm, were prepared by melt spinning in a highly pure helium atmosphere at a wheel surface velocity of $v_s = 30\,\mathrm{m\,s^{-1}}$. Amorphous ribbons fabricated by this technique were crystallized by annealing for 15 min at different temperatures. The crystalline structure and phase composition were analysed by means of x-ray diffraction (XRD) with Cu Kα radiation. Magnetic measurements in the temperature range between 150 K and 550 K were performed using a vibrating sample magnetometer equipped with a 7 T superconducting magnet. The microstructure was studied by use of transmission electron microscopy (TEM, Philips CM200).

3. Results and discussion

3.1. Crystal structure and microstructure

The XRD investigation shows that as-quenched ribbons are amorphous. It has been found that a disordered 1:7 phase with $TbCu_7$-type structure is developed. The results have been published elsewhere [15]. After annealing at temperatures above 1023 K, a 2:17 phase with Th_2Zn_{17}-type structure is formed; after annealing at temperatures higher than 1173 K, α-Fe segregates. In this work, all the samples annealed around 1073 K, which consist of the 2:17 phase, are selected to study the effect of additives. Comparing the XRD patterns of all samples, it was found that the reflection peaks of the Th_2Zn_{17} structure do not shift and, thus, that the lattice parameters keep constant with $a = 8.74$ Å, $c = 12.58$ Å.

Figure 1 presents comparatively the TEM micrographs of the M-free (a) and Zr-containing (b) ribbons. The TEM observations indicate that the grain sizes of all samples are in the range of 50–200 nm.

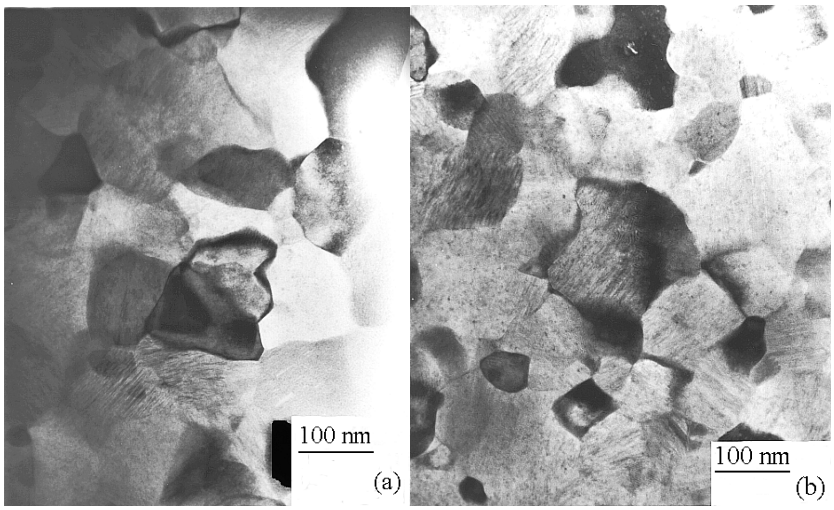

Figure 1. The TEM micrographs of the M-free (a) and Zr-containing (b) ribbons.

3.2. The intrinsic properties

The Curie temperature of the selected $Sm_2Fe_{15}Ga_2C_3$ and $Sm_2Fe_{15}Ga_2C_3M_{0.2}$ (M = Nb, Zr and Cu) ribbons have been measured in a magnetic field of 0.01 T. For all the four samples, the Curie temperature shows the same value of $T_C = 624$ K. In previous works [16, 17], it has been shown that for the composition $Sm_2Fe_{15}Ga_2C_3$ the Curie temperature of the 2:17 phase is not sensitive to small variations in the concentration of gallium and carbon. From geometrical and electronic considerations, it is expected that M elements will occupy Fe or Ga rather than Sm positions. Accordingly, no change in T_C for small amounts of additives is expected.

The anisotropy constants K_1 and K_2 can be determined from fits of the recoil curves of the isotropic polycrystalline samples [18]. The exchange interaction between neighboring grains can be neglected in the case of big enough grain sizes [19]. Hence, the spontaneous magnetic polarization, J_s, is approximately twice the measured remanence J_r. The total free energy, Φ_t, is given by the sum of the crystalline anisotropy energy and the magnetostatic energy:

$$\Phi_t = K_1 \sin^2\theta + K_2 \sin^4\theta - J_s H \cos(\varphi - \theta) \tag{1}$$

where θ denotes the angle between the spontaneous J_s and the c-axis, and the angle between the applied magnetic field H and the c-axis. The c-axis of the crystalline grains is assumed to be randomly distributed around all directions. The recoil curve at a certain temperature is fitted by the minimization of the total free energy for every experimental point.

The anisotropy constants evaluated by this method are illustrated in figure 2. K_1 is observed to decrease more slightly than K_2 with increasing temperature and, in the temperature range 150–250 K, greater K_2 values than K_1 exist. The results of the present work are very similar to those reported for $Sm_2Fe_{17}N_x$ compounds [20–23], which are supported by crystalline electric field calculations [13]. This agreement deals with the similarity of the crystalline structure between $Sm_2Fe_{17}N_x$ and $Sm_2Fe_{15}Ga_2C_3$ compounds. However, negative K_2 values are reported for $Sm_{2+\delta}(Fe_{15}Ga_2C_2$ compounds [24].

The dependence of the spontaneous polarization on the temperature for all selected ribbons, as obtained from $J_s = 2J_r$, is shown in figure 3. The spontaneous polarization shows the same behaviour for all samples. It decreases monotonically with increasing temperature and will drop to zero at the Curie temperature (typically 624 K).

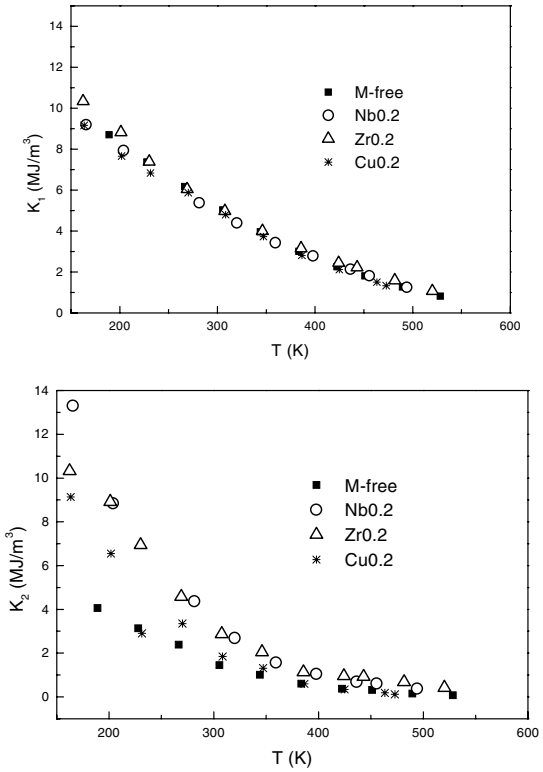

Figure 2. Anisotropy constants determined by fitting the recoil curves.

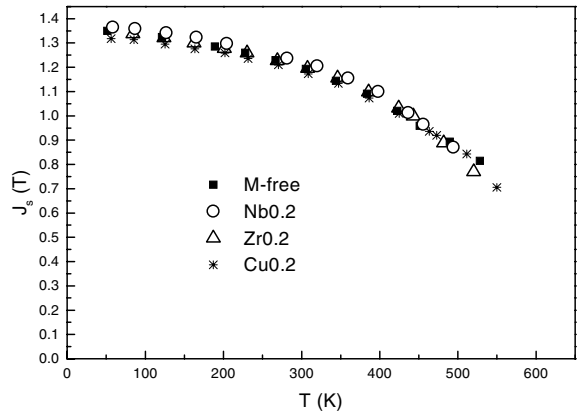

Figure 3. Temperature dependence of the saturation polarization.

The anisotropy constants K_1 and K_2, the spontaneous polarization J_s and the anisotropy field $H_a = (2K_1 + 4K_2)/J_s$ at room temperature are summarized in table 1. All additions enhance the anisotropy field at room temperature. In contrast to the Curie temperature, for the composition $Sm_2Fe_{15}Ga_2C_3$ the anisotropy field of the 2:17 phase is sensitive to small variations of gallium concentrations [17, 18]. The high value of H_a for the Zr case

Table 1. Some intrinsic parameters of $Sm_2Fe_{15}Ga_2C_3M_{0.2}$ compounds at room temperature.

Compounds	K_1 (MJ m^{-3})	K_2 (MJ m^{-3})	J_s (T)	$\mu_0 H_a$ (T)	γ_B (mJ m^{-2})
$Sm_2Fe_{15}Ga_2C_3$	5.0	1.4	1.12	13.4	19.5
$Sm_2Fe_{15}Ga_2C_3Zr_{0.2}$	4.9	2.8	1.12	18.7	20.8
$Sm_2Fe_{15}Ga_2C_3Nb_{0.2}$	4.4	2.6	1.12	16.8	19.8
$Sm_2Fe_{15}Ga_2C_3Cu_{0.2}$	4.7	1.8	1.02	16.3	19.4

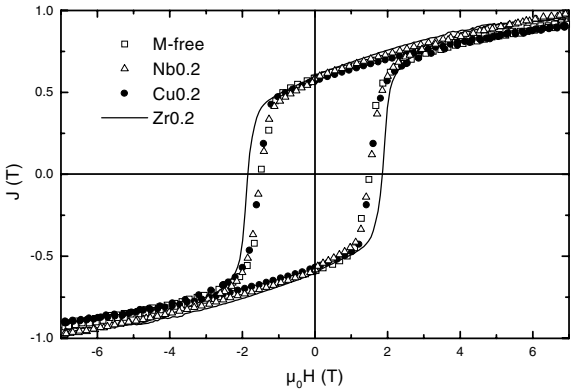

Figure 4. The room temperature hysteresis loops of all samples.

in comparison with the other two additives is particularly striking. This can be interpreted by a different substitution position of Zr in the 2:17 phase as compared to Nb and Cu. Recently, investigations show that for $R_2Fe_{17-x}Ga_x$ compounds, Ga atoms occupy the 18h site at low Ga concentration [25, 26]. This preferential occupancy leads to an increase of the magnetocrystalline anisotropy field. The similarity between $Sm_2Fe_{17-x}Ga_xC_y$ and $R_2Fe_{17-x}Ga_x$ compounds allows us to assume that the increase of the anisotropy for M-added samples and the difference between the Nb (Cu) case and Zr case is due to the different occupation of the additive atoms. As mentioned, from geometrical and electronic considerations, it is expected that M-elements will occupy Fe or Ga positions. It could be assumed that Zr could enter mainly in 6c or 18h positions; meanwhile Cu and Nb will randomly replace Fe or Ga atoms.

3.3. Hard magnetic properties at room temperature

Figure 4 shows the room temperature hysteresis loops of all samples. It can be noticed that for all samples the remanence keeps essentially constant at a common value of $J_r \sim 0.6$ T. On the other hand, different values of the coercivity are observed depending on the nature of the additive. In the case of Cu and Nb, the coercivity exhibits very similar values to that of the M-free sample. In contrast, for Zr addition a significant enhancement of the coercivity field is observed. This fact is related to the influence of additives on the intrinsic properties as well as the microstructure. Consequently, the maximum energy product does not vary notably with Nb and Cu addition in comparison with the M-free ribbon, whereas an important improvement of this property is found for the Zr case. A high $(BH)_{max}$ value of 67 kJ m^{-3} with a coercivity of 1.9 T is achieved for the Zr-containing sample.

3.4. Coercivity mechanism analysis

3.4.1. The critical single domain size. Generally speaking, in multidomain grains magnetization reversal occurs through the nucleation and motion of domain walls; but for single domain materials, the magnetization reversal occurs by nucleation. Therefore, to determine whether the material is a single domain material can give an insight into the coercivity mechanism. The critical diameter of single domain particles D_c can be estimated from the equation $D_c = 9\gamma_B/2\pi M_s^2$, where M_s is the spontaneous magnetization, γ_B denotes the wall energy density, which is given by

$$\gamma_B = 2\sqrt{AK_1}\left(1 + \frac{k+1}{\sqrt{k}}\left(\arcsin\sqrt{\frac{k}{k+1}}\right)\right) \qquad \text{with } k = \frac{K_2}{K_1}. \tag{2}$$

Concerning the evaluation of the exchange constant A, the Weiss molecular field theory states that this parameter is proportional to the Curie temperature. The exchange constant of $Sm_2Fe_{17}N_y$ [23] has a value of $A = 4.8 \times 10^{-12}$ J m^{-1} with a Curie temperature of 750 K. As the $Sm_2Fe_{15}Ga_2C_3M_{0.2}$ compounds have the same crystalline structure as $Sm_2Fe_{17}N_y$, an exchange constant of $A = 4 \times 10^{-12}$ J m^{-1} for $Sm_2Fe_{15}Ga_2C_3$ and $Sm_2Fe_{15}Ga_2C_3M_{0.2}$ compounds can be estimated. The room temperature values of the wall energy density γ_B established by equation (2) are given in table 1. The critical diameter D_c of $Sm_2Fe_{15}Ga_2C_3M_{0.2}$ single domain particles at room temperature is found to be around 350 nm. The average grain size of the 2:17 phase for the selected samples lies within the range of 50–200 nm, which is smaller than the critical diameter of the single domain particle. Therefore, it can be concluded that the 2:17 type magnets are single domain materials. Consequently, it is expected that the nucleation process plays a leading role in determining the coercivity of these ribbons.

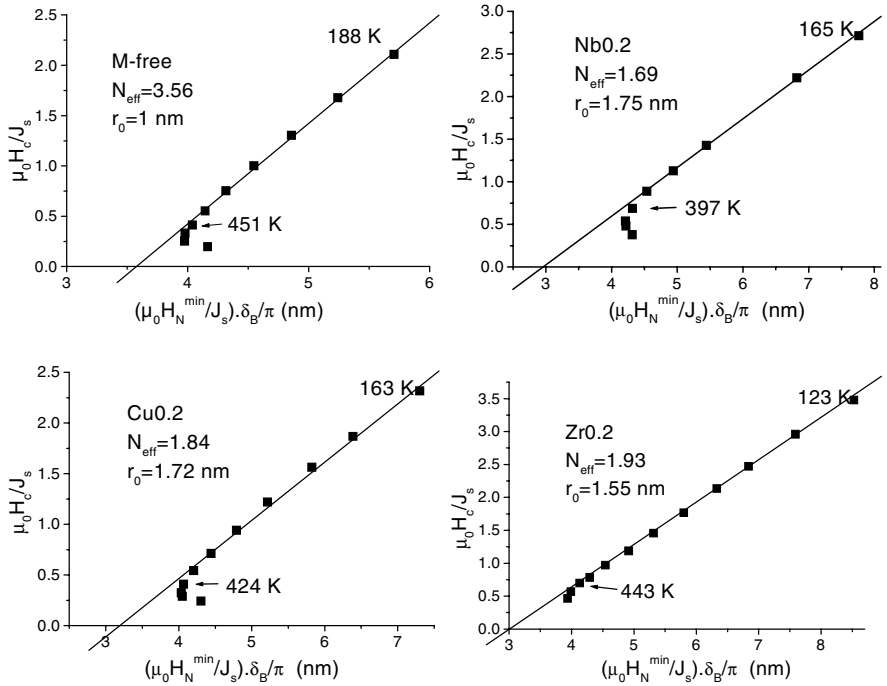

Figure 5. $\mu_0 H_c/J_s$ against $\mu_0 H_N^{min}\delta_B/J_s\pi$ for all samples.

3.4.2. Nucleation. According to the nucleation model [1–6], the coercivity of a real magnet is given by

$$H_c = \alpha_k H_N^{min} - N_{eff} M_s. \tag{3}$$

The microstructural parameter N_{eff} indicates the reduction of the coercivity due to the local demagnetization field at grain edges. α_k describes the coercivity reduction due to the defects at the grain surface. If the change of the crystal anisotropy constant K_1 within a planar grain surface can be described by a $1/ch^2(r/\delta_B)$ function, α_k is given by [3]

$$\alpha_k = 1 - \frac{1}{4\pi^2}\frac{\delta_B^2}{r_0^2}\left(1 - \sqrt{1 + \frac{4\Delta K r_0^2}{A}}\right)^2 \tag{4}$$

where r_0 is the half width of the inhomogeneous grain boundary, ΔK denotes the decrease of K_1 within the inhomogeneity and δ_B is a fictitious wall width of the material. This fictitious wall width can be evaluated as

$$\delta_B = \pi\sqrt{\frac{A}{(K_1 + K_2)}} \tag{5}$$

where A is the exchange constant and K_1, K_2 are the anisotropy constants of the bulk material. Equation (4) is a quite complicated expression to analyse the experimental results. Assuming $\Delta K = K_1$, for intermediate inhomogeneities, i.e., $2\pi r_0 \geqslant \delta_B$, an approximate expression for α_k can be derived:

$$\alpha_k \approx \frac{\delta_B}{\pi r_0}. \tag{6}$$

H_N^{min} is called the minimum nucleation field for randomly oriented grains. Under the conditions $K_1 > 0$ and $K_1 > 4K_2$, H_N^{min} can be approximately derived by $H_N^{min} = (K_1 + K_2)/J_s$. Otherwise, it is determined by

$$H_N^{min} = \frac{1}{2\sqrt{2}J_s}\left\{K_1 + \frac{K_2}{4}\left(W - \frac{K_1}{K_2} + 3\right)\right\}\sqrt{\left(W\left(\frac{K_1}{K_2} + 1\right) - \left(\frac{K_1}{K_2}\right)^2 - \frac{2K_1}{K_2} + 3\right)}$$

with

$$W = \sqrt{\left(\frac{K_1}{K_2} + 1\right)^2 + 8}. \tag{7}$$

In the case of this investigation, the condition $K_1 > 4K_2$ does not hold (figure 2) and H_N^{min} must be calculated from equation (7).

Then, by plotting $\mu_0 H_c/J_s$ against $\mu_0 H_N^{min}\delta_B/J_s\pi$ for different temperatures the unknown parameter r_0, which is a measure of the width of the inhomogeneous grain boundary, can be determined from the inverse slope. This representation is shown in figure 5 for all selected samples. It can be seen that below about 400 K a good linear behaviour between $\mu_0 H_c/J_s$ and $\mu_0 H_N^{min}\delta_B/J_s\pi$ exists, which means that below 400 K the coercivity is dominated by a nucleation process. The deviations at temperature above 400 K could be due to the effect of domain wall pinning. From the straight line, the r_0 and N_{eff} values are obtained and are included in figure 5. According to the meaning of r_0 as a half width of the inhomogeneous grain boundary [3], it can be concluded that the total width of soft magnetic nucleation regions amounts to about 2–3 nm. The value of r_0 relates directly to the value of α_k: a narrow inhomogeneous region means a large α_k. The α_k calculated by equation (6) using the corresponding r_0 are given in figure 6. For all samples, owing to the thick inhomogeneous

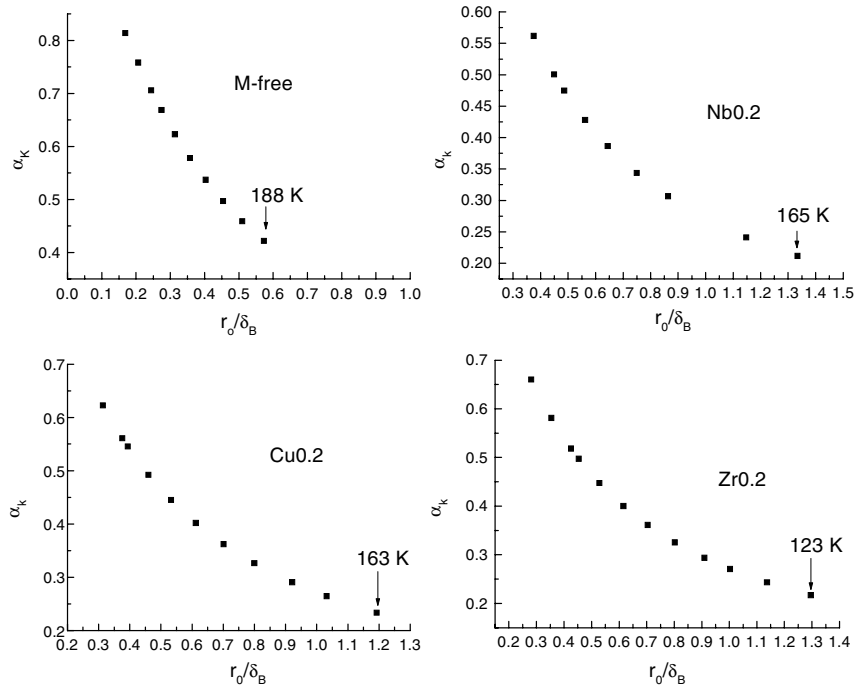

Figure 6. The microstructure parameter α_k as a function of r_0/δ_B.

region α_k have low values. Particularly, additives result in a worse grain surface and cause a reduction of α_k. From this point of view, additives are not favourable to increase the coercivity. The effective demagnetizing factor N_{eff}, which describes the local demagnetizing effect, is in the range of 1.69–3.56. In addition, an inverse dependence between N_{eff} and r_0 is found, which indicates a proportional relation between α_k and N_{eff}. A similar behaviour is reported between α_k and N_{eff} for sintered PrFeB magnets [7]. A brief explanation could be related to the inhomogeneous magnetically soft region within the grain surface. The reduction of the α_k is due to the presence of a soft magnetic region within the grain surface, but meanwhile the magnetic soft region smooths the distribution of the surface charge and leads to a reduction of N_{eff}. From this point of view, additives are beneficial to achieve high coercivities. In conclusion, Zr addition improves the coercivity to 1.9 T from 1.5 T for the M-free sample; Nb and Cu additions do not change it.

3.4.3. Temperature dependence of the magnetic hardening mechanism. From the analysis above, it can be concluded that the coercivity mechanism in melt-spun $Sm_2Fe_{15}Ga_2C_3M_{0.2}$ materials above 400 K cannot be described by the nucleation model. Therefore the pinning model may be considered for this temperature range. As shown in previous papers, the grain boundaries of other magnetic properties than the matrix grains can be considered as strong planar pinning centres. Assuming the thickness of the planar defect r_0 is smaller than the domain wall width, δ_B, of the matrix material, the coercivity is given by [27–30]

$$H_c = \frac{\pi}{3\sqrt{3}} \frac{2K_1}{M_s} \frac{d}{\delta'_B} \left| \sum_{i=1}^{n} \left(\frac{A}{A^{i,i+1}} - \frac{K_1^i}{K_1} \right) \right| - N_{eff} M_s \tag{8}$$

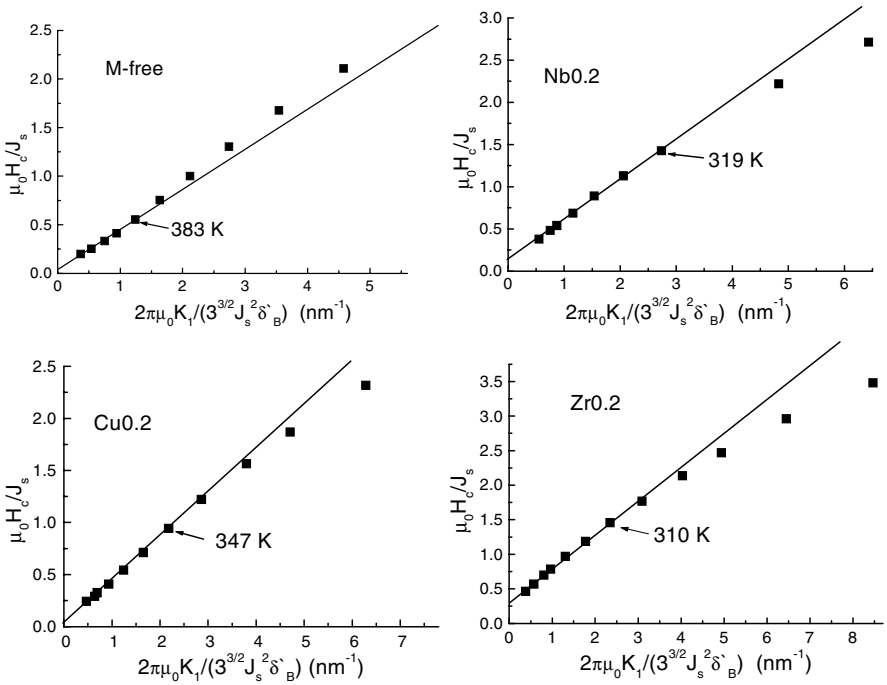

Figure 7. $\mu_0 H_c/J_s$ against $2\pi\mu_0 K_1/3\sqrt{3}J_s^2\delta_B$, as a test for the pinning model.

where n is the number of atomic layers the defect contains, d is the space distance between the layers and $A^{i,i+1}$ and K_1^i denote the exchange constant and anisotropy constant of the ith layer, respectively. Under the assumption that the planar defect is composed of three interlayer distances, within two perturbed lattice planes, K_1 has the common reduced values of 0.5 K_1 and A keeps constant, a value of 1 can be derived from the term $|\sum_{i=1}^{n}(A/A^{i,i+1} - K_1^i/K_1)|$ $= (A/A - 0.5K_1/K_1) + (A/A - 0.5K_1/K_1) = (1 - 0.5) + (1 - 0.5) = 1$. Then equation (8) gives

$$H_c = \frac{2K_1}{M_s}\frac{\pi d}{3\sqrt{3}\delta_B} - N_{eff}M_s. \tag{9}$$

In order to test whether the domain wall is pinned by thin planar inhomogeneities in melt-spun $Sm_2Fe_{15}Ga_2C_3M_{0.2}$ materials, the plots of $\mu_0 H_c/J_s$ against $2\pi\mu_0 K_1/3\sqrt{3}J_s^2\delta_B$ are given in figure 7. It turns out that a linear relation exists above 350 K for all selected samples. The distance of the atomic layers, d, can be determined by the slope of the straight line and a value of 4 Å for all samples is obtained, which is the typical atomic distance in the Th_2Zn_{17} structure. The width of effective inhomogeneities here are obtained as $r_0 = 3 \times 4$ Å $= 12$ Å, which is in good agreement with the value obtained by the nucleation model. The value of α_k obtained from $2\pi r_0/3\sqrt{3}\delta_B$ at 350 K is about 0.2, as expected, which is smaller than the minimum value for the nucleation process. With increasing temperature α_k decreases even further. The effective demagnetizing factor N_{eff} lies around zero or even is negative. As noted by Givord [31], this means that the magnetic inhomogeneities in pinning-type magnets enhance the coercivity whereas for nucleation-type magnets the coercivity is reduced by these inhomogeneities. It can be concluded that the pinning process might control the magnetization reversal process for temperatures above 350 K.

4. Conclusion

All additives enhance the anisotropy field. Particularly, the Zr-added sample has the highest anisotropy field in comparison to the additives of Nb and Cu. The magnetic hardening mechanism at low temperatures is dominated by the nucleation processes in magnetically inhomogeneous regions, whereas at high temperatures (above 350 K) the pinning of the domain walls by grain boundaries controls the coercivity mechanism. From the analysis, it is concluded that the additives deteriorate the grain surface, which is not beneficial for the coercivity.

References

[1] Kronmüller H 1991 *Supermagnets, Hard Magnetic Materials* ed G J Long and F Grandjean, p 461
[2] Kronmüller H, Durst K and Martinek G 1987 *J. Magn. Magn. Mater.* **69** 149
[3] Kronmüller H 1987 *Phys. Status Solidi* b **144** 385
[4] Kronmüller H, Durst K D and Sagawa M 1988 *J. Magn. Magn. Mater.* **74** 291
[5] Kronmüller H, Durst K D, Hock S and Martinek G 1988 *J. Physique Coll.* **49** C8, 623
[6] Martinek G and Kronmüller H 1990 *J. Magn. Magn. Mater.* **86** 177
[7] Kou X C, Kronmüller H, Givord D and Rossignol M F 1994 *Phys. Rev.* B **50** 3849
[8] Kronmüller H, Fischer R, Seeger M and Zern A 1996 *J. Phys. D: Appl. Phys.* **29** 2274
[9] Shen B G, Kong L S, Wang F W and Cao L 1993 *Appl. Phys. Lett.* **63** 2288
[10] Hadjipanayis G C, Zheng Y H, Marthy A S, Gong W and Yang F M 1995 *J. Alloys Compounds* **222** 49
[11] Cao L, Handstein A, Grünberger W, Edelman J, Schultz L and Müller K H 1996 *Appl. Phys. Lett.* **68** 129
[12] Ding J, Street R and McCormick P G 1992 *J. Magn. Magn. Mater.* **115** 211
[13] Kou X C, Qiang W J, Kronmüller H and Schultz L 1993 *J. Appl. Phys.* **74** 6791
[14] Shen B G, Zhang H W, Zhang S Y and Cheng Z H 1999 *Adv. Mater.* **11** 1110
[15] Zhang J X, Kleinschroth I, Cuevas F, Cheng Z H and Kronmüller H 2000 *J. Appl. Phys.* **88** 6618
[16] Cheng Z H, Shen B G, Wang F W and Zhang J X 1994 *J. Phys.: Condens. Matter* **6** L185
[17] Cheng Z H 1995 *PhD Thesis* Institute of Physics, Chinese Academy of Sciences, Beijing
[18] Durst K-D, Kronmüller H and Köhler D 1986 *J. Magn. Magn. Mater.* **59** 86
[19] Köhler D 1992 *PhD Thesis* University Stuttgart
[20] Brennan S, Skomsk1 R, Schedulko N A and Coey J M D 1994 *Proc. 8th Int. Symp. on Magnetic Anisotropy and Rare Earth-Transition Metal Alloys (Birmingham, 1994)* p 71
[21] Wolf M, Wirth S, Wendhausen P A P, Eckert D and Müller K H 1995 *J. Magn. Magn. Mater.* **144** 995
[22] Kim D H, Kim T K, Park W S and Kim Y B 1996 *J. Magn. Magn. Mater.* **163** 373
[23] Kleinschroth I 1997 *PhD Thesis* University Stuttgart
[24] van Lier J, Seeger M and Kronmüller H 1997 *J. Magn. Magn. Mater.* **167** 43
[25] Zhang Y D, Budnick L, Hines W A, Shen B G and Cheng Z H 1999 *J. Appl. Phys.* **85** 4663
[26] Cheng Z H, Shen B G, Wang F W and Kronmüller H 1999 *Appl. Phys. Lett.* **74** 1320
[27] Kronmüller H 1983 *Proc. 7th Int. Workshop on Re-Co-Permanent Magnets (Beijing, 1983)* ed Xiaoshuo Pan, Wenwang Ho and Chengzhou Yu, p 339
[28] Kronmüller H 1978 *J. Magn. Magn. Mater.* **7** 341
[29] Hilzinger H R and Kronmüller H 1975 *Phys. Lett.* A **51** 59
[30] Kronmüller H and Hilzinger H R 1973 *Int. J. Magn.* **5** 27
[31] Givord D, Lu Q, Rossingnol M F, Tenaud P and Viadieu T 1990 *J. Magn. Magn. Mater.* **83** 183